Antiviral Research 192 (2021) 105121

Contents lists available at ScienceDirect

Antiviral Research

journal homepage: www.elsevier.com/locate/antiviral

The novel therapeutic target and inhibitory effects of PF-429242 against Zika virus infection

Sandra Kendra Raini [a], Yuki Takamatsu [b], Shyam Prakash Dumre [c], Shuzo Urata [d], Shusaku Mizukami [e], Meng Ling Moi [a], Daisuke Hayasaka [f], Shingo Inoue [a], Kouichi Morita [a,**], Mya Myat Ngwe Tun [a,*]

[a] Department of Virology, Institute of Tropical Medicine and Leading Program, Graduate School of Biomedical Science, Nagasaki University, 1-12-4 Sakamoto, Nagasaki, 852-8523, Japan
[b] Department of Virology 1, National Institute of Infectious Diseases, 4-7-1 Gakuen, Musashimurayama City, Tokyo, 208-0011, Japan
[c] Central Department of Microbiology, Tribhuvan University, Kirtipur, Kathmandu, Bagmati, 44601, Nepal
[d] National Research Center for the Control and Prevention of Infectious Diseases (CCPID), Nagasaki University, 1-12-4 Sakamoto, Nagasaki, 852-8523, Japan
[e] Department of Immune Regulation, Shionogi Global Infectious Diseases Division, Institute of Tropical Medicine, Nagasaki University, 1-12-4 Sakamoto, Nagasaki, 852-8523, Japan
[f] Laboratory of Veterinary Microbiology, Joint Faculty of Veterinary Medicine, Yamaguchi University, Yamaguchi, 753-8515, Japan

ARTICLE INFO

Keywords:
Zika virus
PF-429242 inhibitor
Antiviral
Drug discovery
Lipid metabolism

ABSTRACT

Zika virus (ZIKV) is a re-emerging mosquito-borne flavivirus of African origin that is transmitted by Aedes mosquitoes. ZIKV was historically limited to Africa and Asia, where mild cases were reported. However, ZIKV has recently been responsible for major global outbreaks associated with a wide range of neurological complications. Since no antiviral therapy exists for ZIKV, drug discovery research for ZIKV is crucial. Intracellular lipids regulated by sterol regulatory element-binding proteins (SREBPs) are important in flavivirus pathogenesis. PF-429242 has been reported to inhibit the activity of site-1 protease (S1P), which regulates the expression of SREBP target genes. Our primary objective in this study is to elucidate the mechanism of the antiviral activity of PF-429242 against the African genotype ($ZIKV_{MR\text{-}766}$) and Asian genotypes ($ZIKV_{H/PF\ 2013}$ and $ZIKV_{PRVABC59}$) using several primate-derived cell lines. The virus titer was determined via a focus-forming assay; we used flow cytometry to quantify intracellular lipids in ZIKV-infected and mock-treated cells. The PF-429242 molecule effectively suppressed ZIKV infection in neuronal cell lines; T98G, U-87MG, SK-N-SH and primary monocytes cell, indicating that PF-429242 molecule can be used therapeutically. A strong reduction in ZIKV replication was observed at 12 μM and 30 μM in in neuronal cell lines and primary monocytes, respectively. Interestingly, the inhibitory effects of the PF-429242 molecule were observed when it was tested on various ZIKV-lineage infections. Lipid quantification reveals that ZIKV increases lipogenesis in infected cells, while the exogenous addition of cholesterol effectively blocks ZIKV replication. Furthermore, the supplementation of oleic acid increases the ZIKV titer. Fenofibrate, an inhibitor of lipid droplet formation, reduces the ZIKV titer. Collectively, our results demonstrate that the development of antiviral drugs against ZIKV could be based on key regulators of lipid metabolism. In addition, this study reveals that the mechanism of the PF-429242-mediated suppression among flavivirus infections is not entirely identical. Our results warrant further evaluation of PF-429242 as a prospective antiviral drug, given the multiple advantageous properties of this compound, such as its limited toxicity, neuroprotective properties, and broad spectrum of capabilities.

1. Introduction

Zika virus (ZIKV) was first discovered in 1947 in the Zika Forest of Uganda (Schwarz et al., 2016). Historically, the majority of human infections caused by ZIKV have been mild (Song et al., 2017). However, ZIKV has recently caused major outbreaks of international concern

* Corresponding author. Department of Virology, Institute of Tropical Medicine. Nagasaki University, 1-12-4 Sakamoto. Nagasaki City, 852-8523, Japan.
** Corresponding author. Department of Virology, Institute of Tropical Medicine, Nagasaki University, 1-12-4 Sakamoto. Nagasaki City, 852-8523, Japan.
E-mail addresses: moritak@nagasaki-u.ac.jp (K. Morita), myamyat@tm.nagasaki-u.ac.jp (M.M. Ngwe Tun).

https://doi.org/10.1016/j.antiviral.2021.105121
Received 24 March 2021; Received in revised form 11 June 2021; Accepted 15 June 2021
Available online 24 June 2021

associated with severe neurological diseases (Adcock et al., 2017). ZIKV remains a global threat, with a growing risk of spread to immunologically naïve human populations (Lessler et al., 2017). Currently, there is no specific treatment for ZIKV infection (Lessler et al., 2017), showing the urgent need to develop and expedite therapeutic agents for ZIKV infection.

Previous studies have shown that lipids are important in flavivirus pathogenesis (Heaton and Randall, 2011). Therefore, we hypothesise that intracellular lipids are potential anti-ZIKV targets. Sterol regulatory element-binding proteins (SREBPs) are inactive precursor proteins embedded in endoplasmic reticulum membranes that are major regulators of lipid metabolism (Ringseis et al., 2013). Precursor SREBP is catalysed in sequential 2-step proteolytic cleavage by site-1 protease (S1P) to become transcriptionally active in response to cholesterol depletion (Alipour and Hassanabadi, 2012). PF-429242 reportedly inhibits the activity of S1P, thereby suppressing the expression levels of SREBP target genes, which are key regulators of intracellular lipid levels (Uchida et al., 2016). Interestingly, the PF-429242 molecule has also been reported to suppress the replication of other viruses, such as dengue virus (Uchida et al., 2016), severe fever with thrombocytopenia syndrome virus (Urata et al., 2018), Hepatitis C virus (Blanchet et al., 2012), and Lassa virus (Urata et al., 2011).

Although PF-429242 exhibits antiviral activity against a large spectrum of viruses *in vitro*, its mechanism of action against ZIKV replication is not fully understood. Information on its mechanism of action could both accelerate the development of antiviral therapies targeting the viral replication cycle and unveil novel metabolic pathways and the virus–host-specific interactions that are required for ZIKV replication (Rumlová and Ruml, 2020; Kuivanen et al., 2017). Finally, greater research in this field can promote the development of ZIKV-targeted antiviral therapy by providing robust scientific knowledge and data (Teissier et al., 2011). Therefore, we investigate whether PF-429242 has an antiviral effect on ZIKV infection, using several human- and non-human-derived cell lines.

2. Methods

2.1. Cell lines and viruses

We cultured human-and non-human (primate) derived cell lines—namely, cervical (HeLa), neuroblastoma (SK-N-SH), glioblastoma (T98G), liver (HEPG2), renal (HEK293), glioblastoma type-I interferon-deficient (U-87MG), African green monkey kidney-derived (Vero), and hamster (BHK-21)—in MEM, except U-87MG, which was grown in Eagle's Medium supplied by Gibco. All cell lines were grown in media supplemented with 10% foetal calf serum (FCS) and 0.2 mM nonessential amino acids and allowed to grow at 37 °C with 5% CO_2. Human CD14 monocytes (hMoCD14+-PB) (Sigma Aldrich) were cultured in RPMI 1640 with L-Glutamine and HEPES from Gibco. The RPMI media was supplemented with 10% foetal calf serum (FCS), 1% penicillin/streptomycin, 0.2 mM nonessential amino acids and 1% sodium pyruvate. The African genotype ($ZIKV_{MR\text{-}766}$) and Asian genotypes ($ZIKV_{H/PF\ 2013}$ and ZIKV $_{PRVABC59}$) that we used in this study were cultured in C6/36-E2 mosquito cells to generate high-titer working stocks. Viral stocks were stored at −80 °C.

2.2. Compounds

PF-429242, fenofibrate, and lovastatin were supplied by Tocris Bioscience, Cayman Chemical, and Adipogen, respectively. PF-429242 and lovastatin were reconstituted to 10 mM and 12.3 mM, respectively, in dimethyl sulfoxide (DMSO); they were stored at −20 °C until use. Fenofibrate was diluted in DMSO on the same day of use. Oleic acid was purchased from Sigma-Aldrich and Cholesterol lipid concentrate was supplied by (Life Technologies Corporation).

2.3. Viability assay

Cell viability assays were performed using PF-429242 (1–500 μM) in a 2-fold serial dilution. Cells at a density of 2×10^5 cells were incubated with a medium containing PF-429242 in a 96-well plate; they were incubated at 37 °C and 5% CO_2 for 72 h to determine the concentration that causes a 50% reduction in cell survival (CC_{50}). A viral inhibition assay was also conducted in parallel with a cytotoxicity assay, in which the drug was introduced together with ZIKV infection into all cell lines and incubated for 72 h. To determine the CC_{50}, cells were incubated with 0.5 mg/ml of [3-(4, 5-dimethylthiazol-2-yl)-2, 5-diphenyl tetrazolium bromide] MTT and incubated for 4 h at 37 °C and 5% CO_2. The MTT formazan crystals were extracted by adding 80 μl of solubilisation solution. Optical density was measured at a 570-nm reading with a microplate reader (Synergy H1 M, Biotech). Cell toxicity was determined using the following equation: Cell viability (%) = (sample value)/(cell control) × 100. We generated dose-response curves and calculated the CC_{50}. Additionally, culture supernatant was harvested for immunostaining by focus to determine viral inhibition (IC_{50}).

2.4. Focus-forming assay

We used a focus-forming assay to examine viral titerss in Vero cells, as previously described by (Tun et al., 2013), with some modifications. Infected culture fluids were diluted in a 10-fold serial dilution and added to Vero cells in a 96-well plate in duplicate. After 1.5 h, 2% FCS methylcellulose was added and incubated at 37 °C and 5% CO_2. Immunostaining was performed at various time points depending on the subsequent quantification assay. Immunostaining was performed using anti-flavivirus mouse monoclonal antibody 12D11/7E8 as primary antibody, followed by HRP-conjugated goat anti-mouse IgG (106 PU, American Qualex) as secondary antibody. The bound conjugate was visualized by adding substrate 3, 3' diaminobenzidine tetra hydrochloride (DAB, Wako) containing hydrogen peroxide. Foci were counted and expressed as focus-forming units (FFU/ml).

2.5. Time-of-addition studies

Cells at a density of 2×10^5 cells per well were seeded in 24-well plates. After 24 h, cells were infected with $ZIKV_{MR\text{-}766}$ and $ZIKV_{H/PF\ 2013}$ at MOI of 0.1 and treated with the PF-429242 molecule at 3 time points: 24 h before infection, during infection (time = 0 h), and 2.5 h after infection. The viral progeny quantification was performed via the focus-forming assay. Further, we determined the exact time point at which PF-429242 suppressed the ZIKV replication cycle, we treated ZIKV-infected cultured cells with 12 μM of PF-429242 and DMSO as control at different (HPI). Virus titers were quantified at 6, 12, 18, and 24 h.

2.6. Binding and internalisation assay for the PF-429242 molecule

A binding assay was performed based on a study conducted by (Talarico et al., 2005), with some modifications. For both assays, cells were seeded in 24-well plates and infected with $ZIKV_{MR\text{-}766}$ and $ZIKV_{H/PF\ 2013}$ at a MOI of 0.1 in a culture medium containing 12 μM of PF-429242 andDMSO as control for 24 h. Cells were incubated for 1 h at 4 °C for the binding assay, while cells were incubated for 1 h at 37 °C for the virus internalisation assay. Infected culture fluid was discarded after incubation, and the cells were washed twice with cold PBS. Finally, cell lysates for both assays were harvested by Isogen-II (Nippon Gene) for analysis by RT-qPCR.

2.7. Quantitative real-time PCR chain reaction

Total RNA was extracted using the Isogen PB kit; next, 500 ng of total RNA was reverse-transcribed to cDNA using the PrimeScript™ R kit.

Transcribed mRNAs were quantified via SYBR real-time PCR, as described by (Tun et al., 2014). The results of unknown samples were expressed in absolute copy numbers, determined by comparing the threshold curve relative to the standard curve. The standard curve was obtained from serial dilutions of purified cDNA. The primers used in this study are listed in (Xu et al., 2016).

2.8. Infection assay

Cells at a density of 2×10^5 were seeded in 24-well plates. The following day, cells were infected with $ZIKV_{MR\text{-}766}$ and $ZIKV_{H/PF\ 2013}$ at MOI of 0.1 in a culture medium containing 12 μM of PF-429242 or DMSO. Supernatants were collected at different HPIs to analyse viral titers via the focus-forming assay in Vero cells, as described above. For the inhibitor's treatment, cells were seeded in a 24-well plate and following day, infected cells were treated with PF-429242 and incubated for 24 h. After incubation, the culture media were replaced with fresh media containing 40 μM of lovastatin or fenofibrate. The culture supernatant was harvested at 48 HPIs to measure the virus titer via immunostaining, as described above. Intracellular cholesterol was quantified using an Amplex Red Cholesterol assay kit (Invitrogen) according to the manufacturer's instructions.

2.9. Lipid quantification via flow cytometry

Cells at a density of 1×10^6 cells per well were seeded in a six-well plate. Cells were with $ZIKV_{MR\text{-}766}$ and $ZIKV_{H/PF\ 2013}$ at a MOI of 0.1 in a culture medium containing 12 μM of PF-429242 or DMSO as control. After incubation at 37 °C and 5% CO_2 for 24 h, cells were fixed with BD Cytofix/Cytoperm™ solution for 20 min. The cells were then trypsinised and permeabilised with BD perm/wash buffer for 10 min. They were washed twice and stained at 4 °C for 30 min in the dark with BODIPY 493/503 (4, 4-difluoro-1, 3, 5, 7, 8-pentamethyl-4-bora-3a, 4a-diaza-s-indacene). Finally, the cells were washed twice and resuspended in the fluorescence-activated cell-sorting (FACS) buffer for flow cytometry analysis using a FAC scan flow cytometer (BD bioscience). We used Flowjo version 10.6.2 software to determine the percentage of positive cells.

2.10. Immunofluorescence assay

Cells at a density of 1×10^5 were seeded in 8 Well Millicell EZ Slide (Merck Millipore LTD). The following day, cells were infected with $ZIKV_{MR\text{-}766}$ at MOI of 0.1 in presence of 12 μM of the PF-429242 or DMSO for 24 h. Infected cells were then fixed in 4% paraformaldehyde for 30 min, and permeabilized in PBS containing 1% Nonidet P-40 for 30 min. After washing thrice, cells were blocked at room temperature for 30 min. Cells were incubated with 1:500 anti-flavivirus mouse monoclonal antibody 12D11/7E8. The primary antibody was detected by Alexa Fluor 594-anti-mouse IgG antibody (Invitrogen) with 2.5 μM/ml of BODIPY 493/503. Cells were sealed with ImmunoSelect Antifading Mounting Medium (Dianova GmbH) which contained 4', 6-Diamidino-2-phenylindole (DAPI). Images were captured with BZ-X710 fluorescence microscope. Further, the intensity of fluorescence emitted by BODIPY was measured at Ex 485 nm, E 515 nm using Synergy microplate reader (BioTek).

2.11. Statistical analysis

A student's *t*-test was used to determine significant differences between groups. Significant differences among more than two groups were analysed by one-way ANOVA. All statistical comparisons were two sided with ($^*p < 0.05$). The statistical analyses were performed with Prism Software (Graph Pad version 9.0.1[151]).

3. Results

3.1. The effect of PF-429242 against ZIKV infection on various derived cell lines

To gain insight into the antiviral mechanism of the PF-429242 molecule, we infected multiple cell types from several human and non-human primate-derived cell lines with $ZIKV_{MR\text{-}766}$ and $ZIKV_{H/PF\ 2013}$ in a culture medium containing 12 μM of PF-429242 and DMSO as control. Infected culture fluids were collected at 24, 48, and 72 HPIs; viral titers were determined via the focus-forming assay. PF-429242 significantly reduced viral infection in the SK-N-SH, HeLa, T98G, and U-87MG cell lines (Fig. 1A–D), while no inhibition was observed in the BHK, HepG2, HEK-293, and Vero cell lines (Fig. 1 E–H). The initial antiviral effect was observed at 24 HPI in the SK-N-SH, HeLa, T98G, and U-87MG cell lines at a concentration of 12 μM. Next, we evaluated whether higher concentration of 30 μM and 60 μM of the PF-429242 molecule could be sufficient to cause antiviral effect on ZIKV replication in BHK, HepG2, HEK-293, and Vero cell lines. Intriguingly, no antiviral effect was observed in these cell lines. To demonstrate that the PF-429242 molecule can be potentially used therapeutically, we examined the effect of this compound on primary monocytes and it significantly reduced ZIKV replication at a concentration of 30 μM at 72HPI (Fig. 1I).

3.2. The determination of cytotoxicity and inhibitory concentrations of PF-429242

The PF-429242 molecule did not affect cell viability at the concentration up to around 200 μM at 72 HPI. We calculated the following CC_{50} values (Fig. 2A, Table 1): SK-N-SH (CC_{50}: 167.6 μM), HeLa (CC_{50}: 233.4 μM), T98G (CC_{50}: 183.2 μM), and U-87MG (CC_{50}: 216.8 μM). We then determined the CC_{50} of primary monocytes. Our results revealed that primary monocytes were 100% viable at 500 μM at 72 HPI. Moreover, the PF-429242 dose dependently inhibited $ZIKV_{MR766}$ and $ZIKV_{H/PF2013}$ infection (Fig. 2B, Table 1). The IC_{50} values were 13.3 μM for SK-N-SH, 6.3 μM for HeLa, 6.9 μM for T98G, and 14 μM for U-87MG in the $ZIKV_{MR766}$ strain. The IC_{50} was 11.9 μM for SK-N-SH, 9.4 μM for HeLa, 3.5 μM for T98G, and 11.7 μM for U-87MG in the $ZIKV_{H/PF2013}$ strain. The cell viability assay indicated that the PF-429242 molecule inhibited $ZIKV_{H/PF2013}$ more efficiently in T98G (SI: 52.3) than in HeLa (SI: 24.8), U-87MG (SI: 18.5), or SK-N-SH (SI: 14.1). On the other hand, PF-429242 inhibited $ZIKV_{MR766}$ most efficiently in HeLa (SI: 37.0), followed by T98G (SI: 26.6), U-87MG (SI: 15.5), and SK-N-SH (SI: 12.6). Finally, a significant concentration-dependent reduction of the ZIKV titer was observed at a low concentration of 3.5 μM in T98G (Fig. 2B, Table 1). The IC_{50} values for Human CD14 monocytes were 70.22 μM in the $ZIKV_{MR766}$ and 51.55 μM in $ZIKV_{H/PF2013}$ strain. The cell viability assay indicated that the PF-429242 molecule inhibited ZIKV more effectively in primary cells compared to secondary cells.

3.3. Time-of-drug-addition assay

To evaluate which phase of the ZIKV replication cycle was impaired by PF-429242, we exposed ZIKV-infected cells to PF-429242 before, during, and after virus infection. We found that—in contrast to the pretreatment of ZIKV-infected cells, which had no profound effect on viral replication (Fig. 3A)—the treatment of ZIKV-infected cells with PF-429242 significantly decreased ZIKV replication when added together with the virus (Fig. 3B) or after virus infection (Fig. 3C). Furthermore, we performed binding and internalisation assays to determine whether PF-429242 inhibited the entry or post-entry stages of virus infection. Briefly, cell lysates of infected cells with $ZIKV_{MR\text{-}766}$ and $ZIKV_{H/PF\ 2013}$ in the presence or absence of PF-429242 were harvested by Isogen-II (Nippon Gene) for analysis using RT-qPCR. We found out that ZIKV viral replication was not reduced (data not shown).

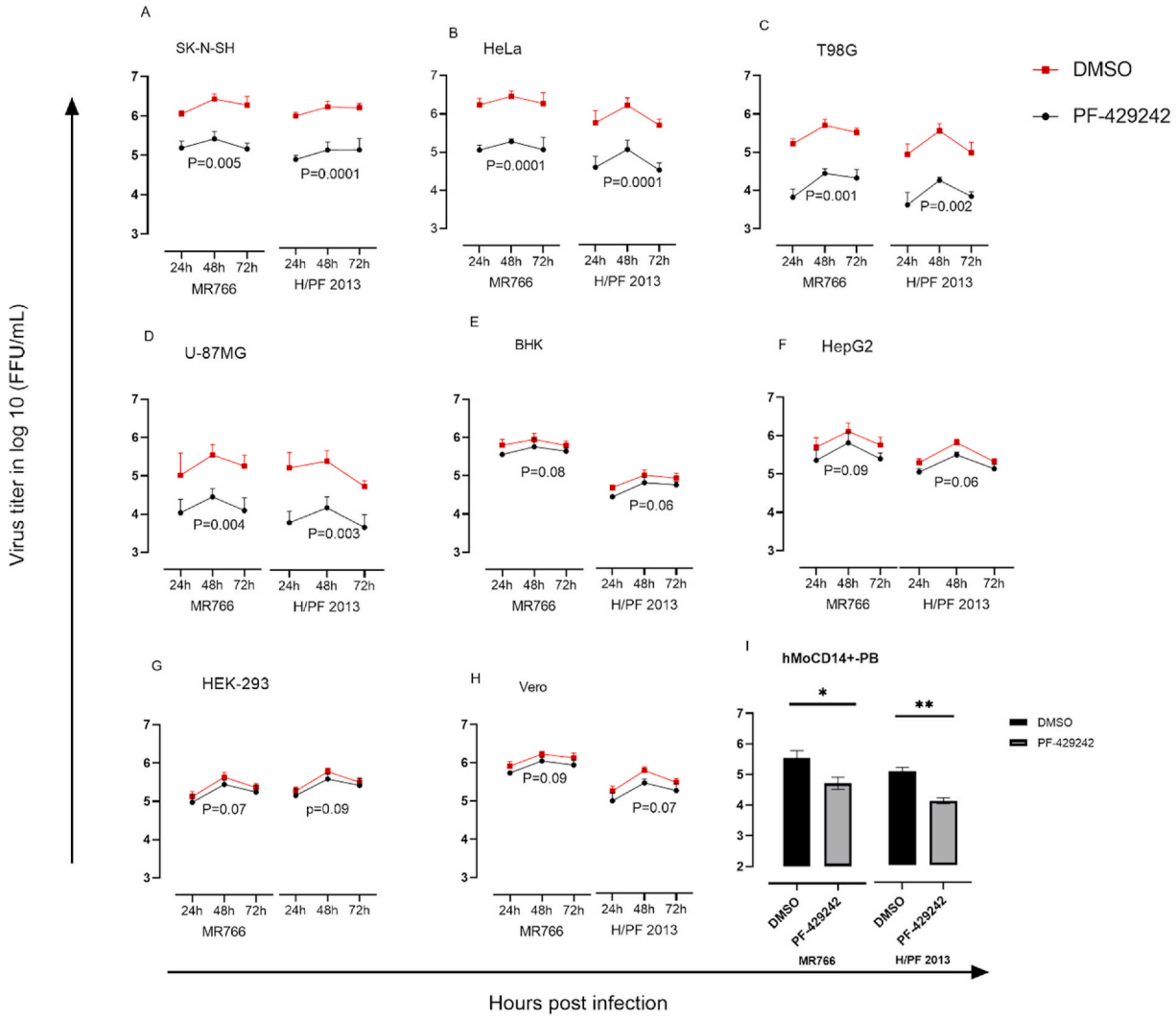

Fig. 1. PF-429242 inhibits ZIKV infection in neuronal and cervical cell lines. SK-N-SH, HeLa, T98G, and U-87MG cells at a density of 2×10^5 cells per well were seeded in a 24-well plate and infected with $ZIKV_{MR\text{-}766}$ and $ZIKV_{H/PF\ 2013}$ at MOI of 0.1 in a culture medium containing 12 μM of PF-429242 or DMSO. The culture supernatants were harvested at 24, 48 and 72 HPIs to measure the virus titer via immunostaining. The PF-429242 molecule successfully suppressed ZIKV infection in the SK-N-SH (A), Hela (B), T98G (C) and U-87MG (D) cell lines, while there was no inhibition in the BHK (E), HepG2 (F), HEK-293 (G), Vero (H) and primary monocytes (I) cell lines. The standard error of the mean (SEM) values of the results from three independent experiments are shown. The calculated p-values are shown on the groups that were compared. Titers are expressed as FFU/ml.

To determine the exact time point at which PF-429242 suppressed the ZIKV replication cycle. Our results reveal that PF-429242 induces a strong reduction in the ZIKV titer from 12 to 18 h in the SK-N-SH, HeLa, T98G, and U-87MG cell lines (Fig. 3D), while there is no antiviral activity against Japanese encephalitis virus (JEV) (Supplementary Fig. 2). Furthermore, we assessed the antiviral effect of PF-429242 against an additional ZIKV strain ($ZIKV_{PRVABC59}$). This drug showed similar ZIKV inhibitory effects against $ZIKV_{PRVABC59}$ infections (Supplementary Fig. 3).

3.4. ZIKV infection increases lipogenesis in infected cells

A strong reduction in ZIKV replication was observed when PF-429242 was added 12–18 h after ZIKV inoculation, indicating that this drug was effective at early stage of the ZIKV replication cycle (Fig. 3D). Previous reports have shown that many viruses, including ZIKV, are dependent on lipid metabolism to support their replication. Since the PF-429242 molecule regulates lipid synthesis, we performed flow cytometry analysis to reveal the effect of this drug on in lipid amount. Our results align with previous findings and further indicate that ZIKV infection increases lipogenesis, as measured by FACS analyses (Fig. 4A). Interestingly, PF-429242 reduced lipids in SK-N-SH, HeLa, T98G, and U-87MG cells infected with $ZIKV_{MR\text{-}766}$ up to 28.14%, 38.52%, 25.61%, and 39.15%, respectively. In these same cell types infected with $ZIKV_{H/PF2013}$, PF-429242 reduced lipids up to 30.35%, 29.99%, 34.77%, and 28.68%, respectively. Statistical analyses are shown in (Fig. 4B). Further, flow cytometry analysis indicated that, lipid amounts were not affected in BHK, HepG2, HEK-293, and Vero cell lines in presence of PF-429242 molecule (Supplementary Fig. 4A and 4B).

3.5. ZIKV differentially alters various classes of lipids

PF-429242 efficiently reduced intracellular cholesterol in SK-N-SH, HeLa, T98G, and U-87MG cells infected with $ZIKV_{MR\text{-}766}$ and $ZIKV_{H/PF2013}$ (Supplementary Fig. 5A and 5B). Thus, we posit that the exogenous addition of cholesterol is essential to maintaining the active replication of ZIKV. To test this possibility, PF-429242-treated infected cells were supplemented with cholesterol lipid concentrate, and infected culture supernatants were harvested for virus quantification. Surprisingly, we found that the exogenous addition of cholesterol lipid

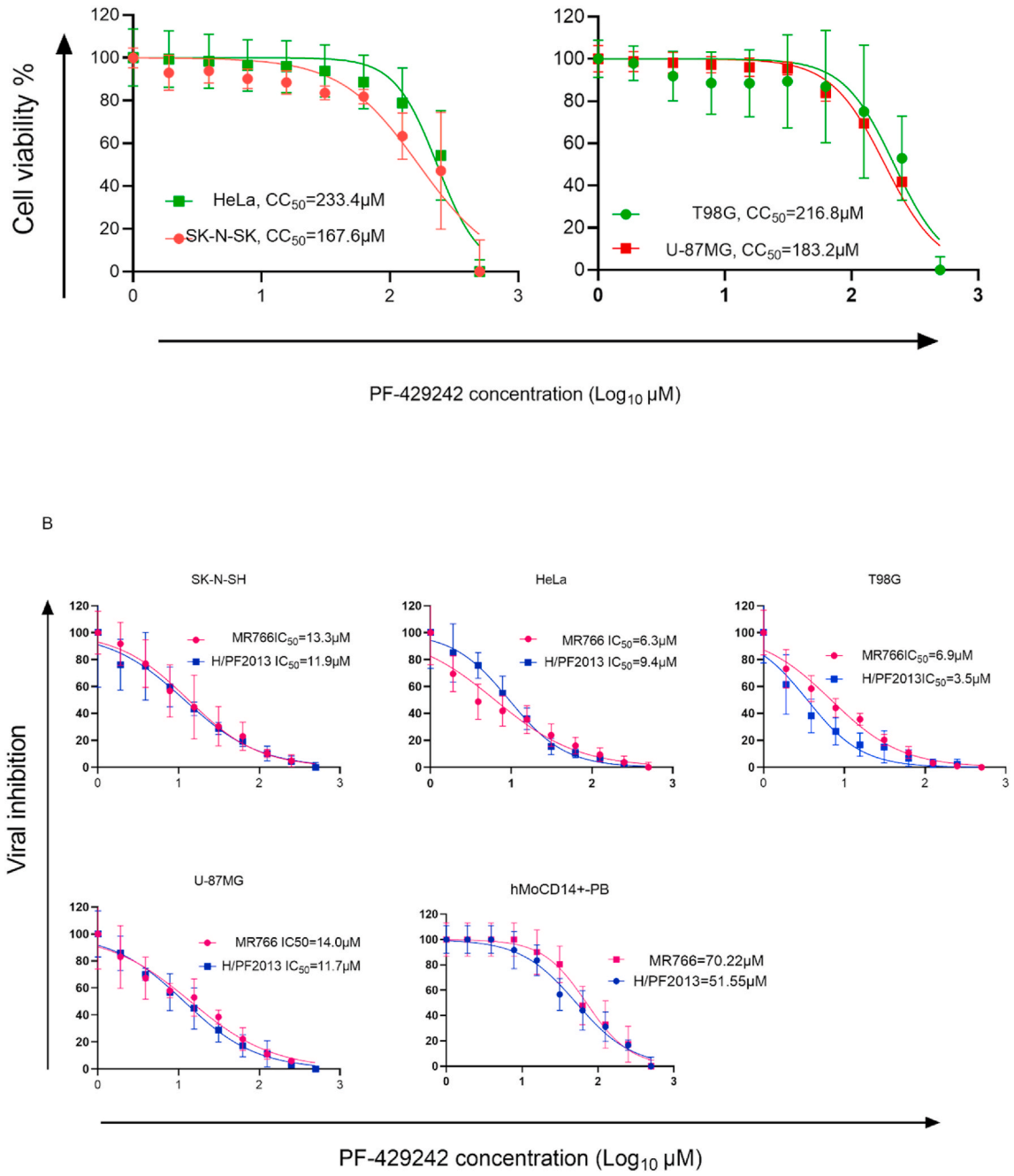

Fig. 2. Dose-response curve for the PF-429242 compound. SK-N-SH, HeLa, T98G, and U-87MG cells at a density of 2×10^5 per well in a 96-well plate were treated with increasing concentrations of PF-429242 to determine the cytotoxicity (CC_{50}) and inhibitory (IC_{50}) concentrations. Intracellular ATP was measured in uninfected cells after 72 h (Fig. 2A). Cells were infected with $ZIKV_{MR\text{-}766}$ and $ZIKV_{H/PF\ 2013}$ at MOI of 0.1 in a culture medium containing PF-429242 or DMSO to determine inhibitory concentrations. The culture supernatants were harvested at 72 HPIs to measure the virus titer (Fig. 2B). The X-axis indicates the concentration of PF-429242 and Y-axis indicates the inhibitory and cytotoxic percentages. The antiviral activity of PF-429242 was calculated (Table 1). The SEM of 3 independent experiments were analysed by the non-linear regression of the dose-response curve.

concentrate resulted in reduced virus production (Fig. 5A). To assess whether the reduction in virus replication was a result of cell cytotoxicity from cholesterol, MTT assay was performed. Our CC_{50} results revealed that all cell types were above 96% viable at the concentration of 500 μM at 24 HPI (Table 2).

Next, infected cells treated with PF-429242 were cultured in the presence of oleic acid. Interestingly, the supplementation of oleic acid in ZIKV-infected cultured cells subsequently led to dose-dependent increases in the ZIKV titer in PF-429242-treated cells (Fig. 5B), as well as an increase in the focus assay titer, as shown in Supplementary Figure 4. To visualize the rescue effect of oleic acid on ZIKV replication, staining and imaging of lipids droplets was performed using IFA. Culturing of infected cells treated with PF-429242 in presence of oleic acid markedly induced lipid droplet abundance which consequently increased ZIKV particles (Fig. 6A). In addition, co-localization of lipid droplet with ZIKV envelope protein was observed (Fig. 6B). Measurement of fluorescent intensity further confirmed these findings in (Fig. 6C).

3.6. Lipid droplet abundance plays an essential role in ZIKV infection

The SREBP-1 pathway activates the transcription of genes that encode triglyceride in response to lipid droplet formation (Urata et al.,

Table 1
Antiviral effects of PF-429242 on various cell lines.

Cell line	IC_{50}μM/mL		CC_{50}	SI[a] $ZIKV_{MR766}$	SI[a] $ZIKV_{H/PF2013}$
	$ZIKV_{MR766}$	$ZIKV_{H/PF2013}$			
SK-N-SH	13.3	11.9	167.6	12.6	14.1
HELA	6.3	9.4	233.4	37.0	24.8
T98G	6.9	3.5	183.2	26.6	52.3
U-87MG	14.0	11.7	216.8	15.5	18.5
hMoCD14+-PB	70.22	51.55	500	7.1	9.7

[a] $SI=CC_{50}/IC_{50}$.

2018). We used chemical inhibitors of the SREBP pathway (fenofibrate and lovastatin) to assess the importance of lipid droplet abundance in ZIKV infection (Supplementary Fig. 6). These statins are FDA-approved for clinical use against hyperlipidaemia (Majeed et al., 2019). The concentrations that caused a 50% reduction in cell viability in the SK-N-SH, HeLa, T98G, and U-87MG cell lines after 24 h of treatment were 63 μM, 87 μM, 71 μM, and 125 μM for fenofibrate, respectively; these concentrations were 81 μM, 79 μM, 95 μM, and 141 μM for lovastatin, respectively (Table 3). Treatment with a fenofibrate inhibitor resulted in a significant reduction in the ZIKV titer (as measured by the focus reduction assay), compared to a lovastatin inhibitor (Fig. 6).

4. Discussion

In this study, we examined the inhibitory effects of the PF-429242 molecule on ZIKV infection. Notably, PF-429242 suppressed viral replication in the SK-N-SH, HeLa, T98G, and U-87MG cell lines (Fig. 1A–D), while no inhibition was observed in the BHK-21, HepG2, HEK-293, and Vero cell lines (Fig. 1E–H). The inhibition of ZIKV in U-87MG cells (Fig. 1D) suggests that the differential suppression of ZIKV in neuronal cell lines (SK-N-SH, T98G, and U-87MG) and cervical cell lines

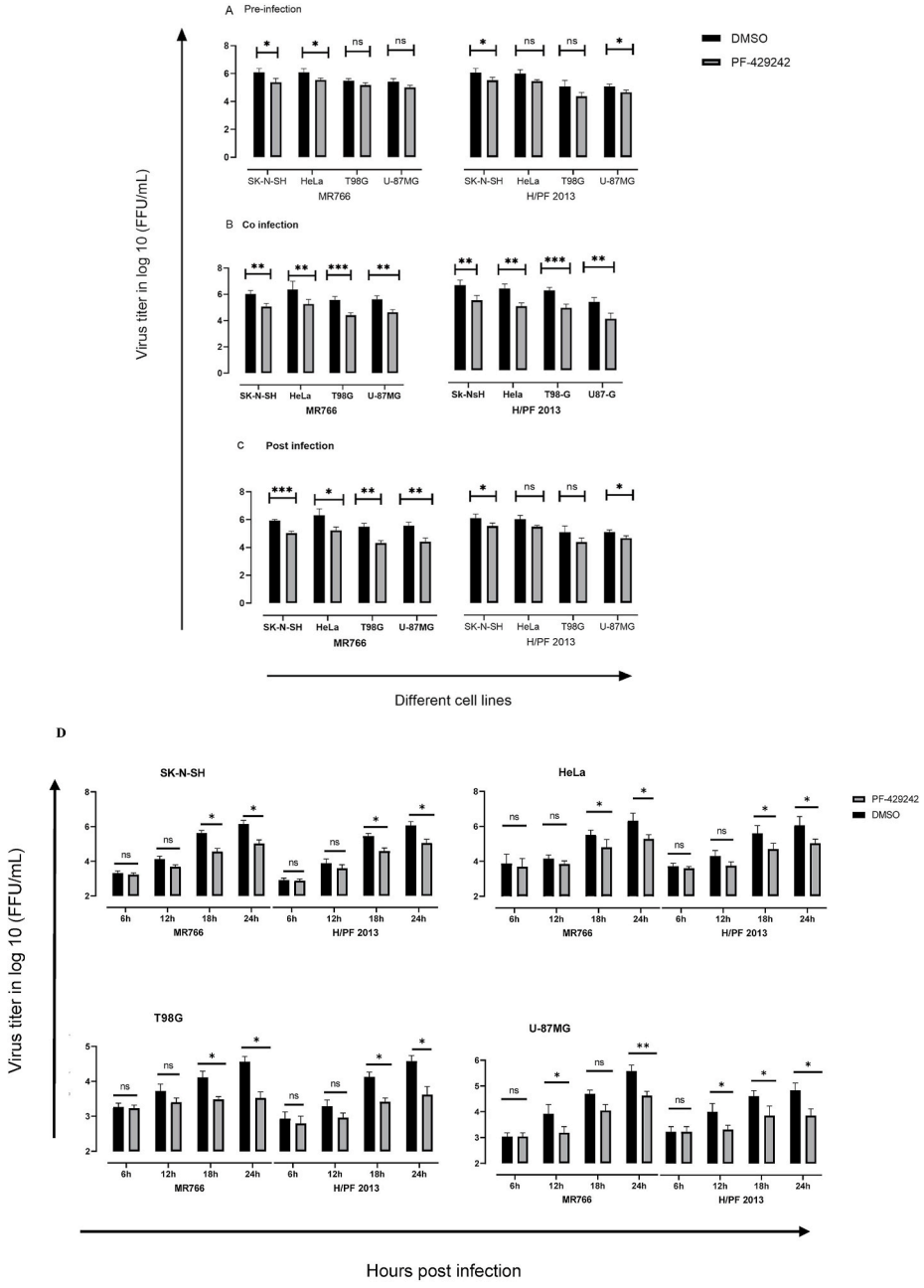

Fig. 3. Time-of-addition studies. SK-N-SH, HeLa, T98G, and U-87MG cells at a density of 2×10^5 per well were seeded in 24-well plates and infected with $ZIKV_{MR-766}$ and $ZIKV_{H/PF\ 2013}$ at MOI of 0.1 before infection (Fig. 3A), during infection (Fig. 3B), and after infection (Fig. 3C). Supernatants were harvested at 24 HPI and analysed via the focus-forming assay. PF-429242 significantly inhibited ZIKV infection from 12 to 18 HPI (Fig. 3D). The asterisks indicate statistical significance in comparison to DMSO, as follows: ns, $P > 0.05$. *, $P < 0.05$; **, P 0.005. ***, $P < 0.001$. The SEM values of the results from three independent experiments are shown.

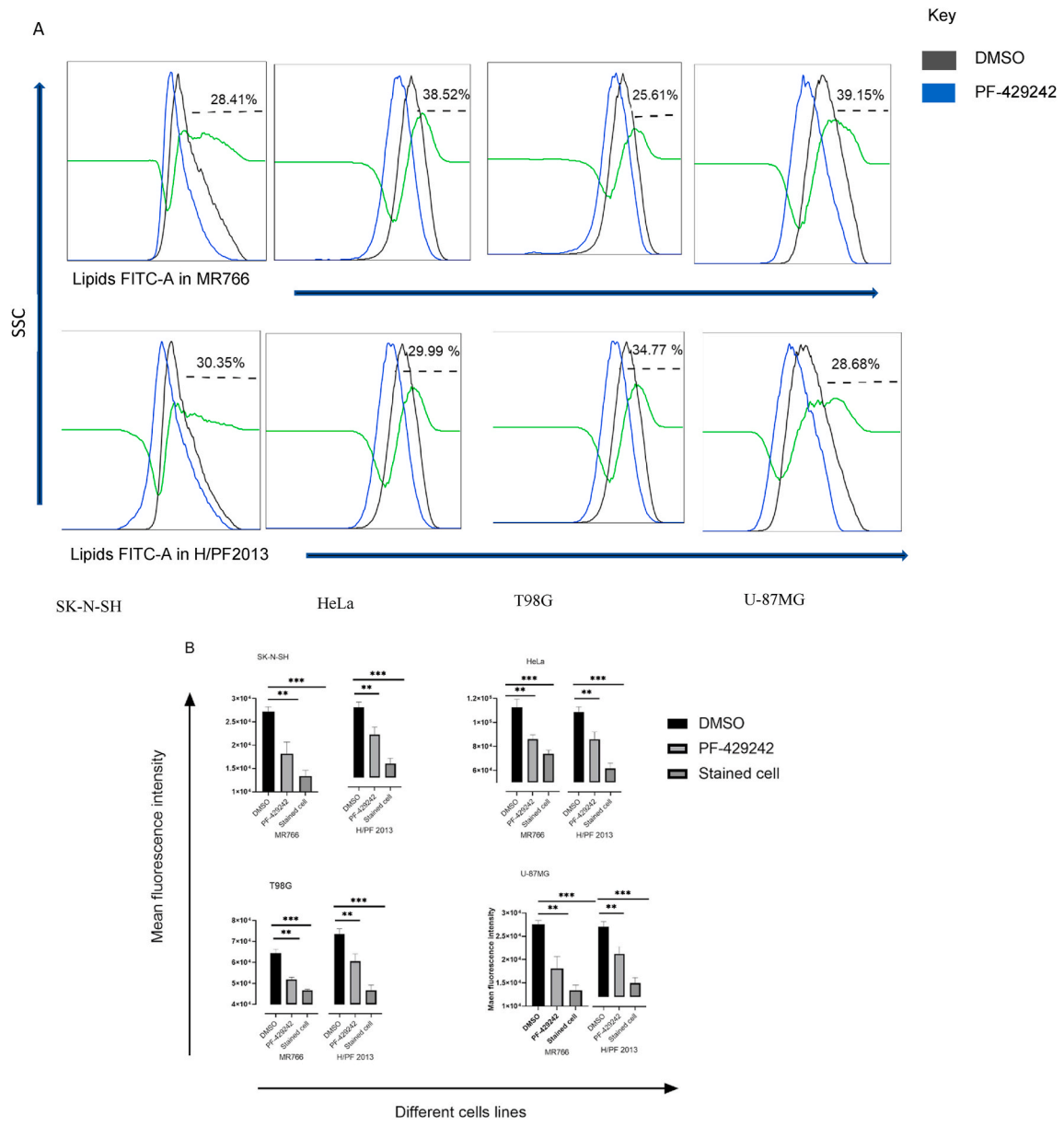

Fig. 4. PF-429242 effectively decreases lipogenesis in infected cells. SK-N-SH, HeLa, T98G, and U-87MG cells at a density of 1×10^6 cells per well were seeded in a six-well plate. Cells were stained with BODIPY and analysed using a FAC scan flow cytometer (BD bioscience). Flowjo version 10.6.2 software was used to determine the percentage of positive cells. Flow cytometry revealed that ZIKV infection increases lipogenesis in cells. Furthermore, this analysis showed that PF-429242 significantly reduced lipogenesis in infected cells (Fig. 4A). Gates were set on stained cells prior further analysis. Histograms are representative flow cytometry data from one experiment from each cell. Statistical analysis of mean fluorescent intensity of three independent experiments was analysed by student *t*-test (Fig. 4B). The asterisks indicate statistical significance in comparison to DMSO, as follows: *, $P < 0.05$; **, P 0.005. ***, $P < 0.001$.

(HeLa) does not result from type-I interferon (IFN) (McNab et al., 2015) but rather from the suppressive effects of PF-429242 on S1P. These observations can be explained by the correlation between the inhibitory effects of the PF-429242 molecule (Supplementary Fig. 1) and flow cytometry analysis results in the BHK-21, HepG2, HEK-293, and Vero cell lines (Supplementary Fig. 4A and 4B) which rules out that the PF-429242 molecule does not inhibit S1P in these cell lines. Most importantly, the fact that PF-429242 reduced ZIKV infection in neuronal and primary cell lines indicates that this compound is a potential anti-ZIKV drug with neuroprotective properties (Miner and Diamond, 2017). Consistent with a study conducted by (Chan et al., 2016), we found out that all cell lines were susceptible to ZIKV infection, which suggests potential animal reservoirs for ZIKV infection.

Compared to chloroquine (Delvecchio et al., 2016) and other anti-ZIKV substances reported by (Balasubramanian et al., 2017), PF-429242 is a potent ZIKV inhibitor, as indicated by the high SI values and the fact that this compound suppressed ZIKV at the low concentration of 3.5 μM (Table 1, Fig. 2B). The effectiveness of the PF-429242 molecule in suppressing ZIKV infection as indicated by the high SI values of primary monocytes cells further demonstrates that this drug can be used therapeutically. We observed that lower doses of the PF-429242 were required to attain 50% inhibition of ZIKV infection in secondary cell lines. The variation in response of these cells to the Pf-429242 could be due to the differences in gene expression and the high passage history. Previous studies have shown differences in gene expression between cells and accumulation of mutations in immortal secondary cells (Arul, 2017). Although PF-429242 did not prevent viral entry into host cells—as demonstrated by the binding and internalisation assays (data not shown)—the treatment of ZIKV-infected cells with PF-429242 significantly decreased ZIKV replication when added together with the

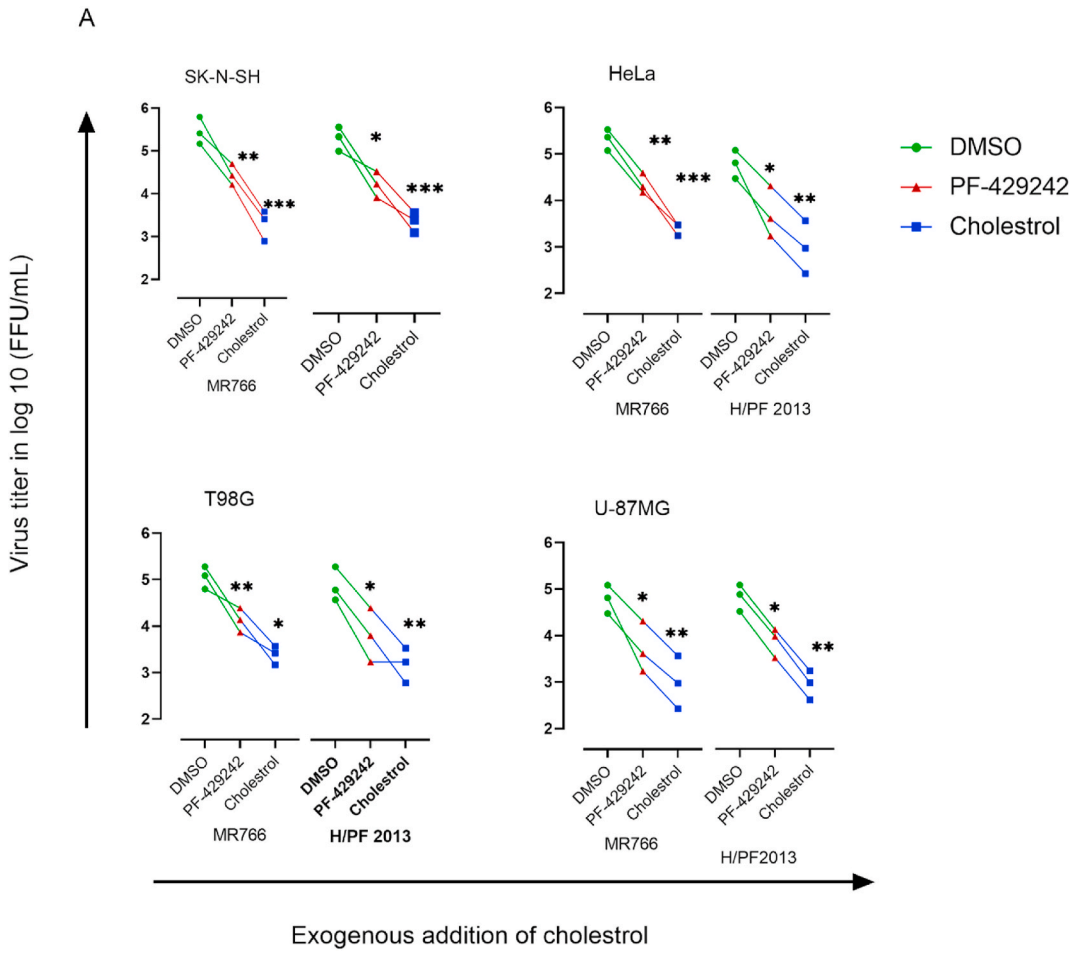

Fig. 5. ZIKV infection differentially alters differ classes of lipids. SK-N-SH, HeLa, T98G, and U-87MG cells at a density of 2×10^5 cells per well were seeded in a 24-well plate and infected with $ZIKV_{MR\text{-}766}$ and $ZIKV_{H/PF\ 2013}$ at MOI of 0.1 in a culture medium containing 12 μM of PF-429242 or DMSO in presence of cholesterol or oleic acid. The culture supernatants were harvested at 24 HPI to measure the virus titer via immunostaining. Exogenous addition of cholesterol in ZIKV infection impaired viral replication in cells (Fig. 5A). Oleic acid supplementation markedly increased viral replication in ZIKV treated cells in a dose dependent manner (Fig. 5B). The asterisks indicate statistical significance in comparison to DMSO, as follows: *, $P < 0.05$; **, P 0.005. ***, $P < 0.001$. The SEM values of the results from three independent experiments are shown.

virus (Fig. 3B) or after virus infection (Fig. 3C). This suggests that PF-429242 may have a potential treatment effect against ZIKV infection (Song et al., 2020). PF-429242 markedly reduced ZIKV replication 12–18 h after inoculation in the SK-N-SH, HeLa, T98G, and U-87MG cell lines (Fig. 3D), suggesting that this compound interferes with ZIKV replication (Chan et al., 2017). In contrast to our findings—which show that the treatment of ZIKV-infected cells with PF-429242 significantly decreases ZIKV replication at 18 HPIs—antiviral activity against Dengue virus (DENV) occurs at 72 HPI (Chan et al., 2017), while there is no antiviral suppression of JEV (Supplementary Fig. 2). The fact that the PF-429242 molecule differentially suppresses flavivirus infections at different time points indicates that the mechanism of the PF-429242-mediated suppression among flavivirus infection is not entirely similar. The differential suppression of flavivirus by PF-429242 could be explained by the fact that JEV belongs to a different clade from DENV and ZIKV as revealed by phylogenetic and molecular analyses (González et al., 2018). In addition, drugs that differentially suppresses viral infection within the group of flavivirus has been reported (Chiu et al., 2018) (Wang et al., 2019). Therefore, in depth studies to understand the antiviral suppression of flavivirus infection at the viral genome level by using tools such as reverse genetics should be conducted (Komoto et al., 2020). Similar ZIKV inhibitory effects of the PF-429242 molecule were observed when it was tested on different ZIKV-lineage infections (Supplementary Fig. 3). This indicates that PF-429242 could help manage recent ZIKV infections caused by pathogenic Asian ZIKV-lineage strains (Simonin et al., 2016).

Flow cytometry analysis revealed increased lipogenesis in infected cells (Fig. 4A). These results corroborate those of previous studies, which have shown that intracellular lipids are important for flavivirus infectivity (Martín-Acebes et al., 2016; Heaton and Randall, 2011). Notably, this compound significantly reduced lipid levels in PF-429242-treated cells (Fig. 4A). These findings align with those of studies conducted by (Merino-Ramos et al., 2017; Blanchet et al., 2015).

In this study, we observed that ZIKV infection differentially altered various classes of lipids. In contrast to previous studies which have shown the importance of cholesterol in flavivirus infections (Osuna-Ramos et al., 2018), our study found out that exogenous addition of cholesterol reduced virus replication (Fig. 5A). This information supports similar findings previously reported by (Lee et al., 2008), who demonstrated that the exogenous addition of cholesterol effectively inhibits dengue virus replication. Additionally, accumulation of cholesterol within the lysosomes has been reported to reduce viral replication (Martín-Acebes et al., 2016). As with other studies conducted by (Hyrina et al., 2017; Ramphan et al., 2017), our results consistently show that oleic acid supplementation increased the ZIKV titer (Fig. 5B). This may result from the inducement of lipid droplet formation by oleic acid

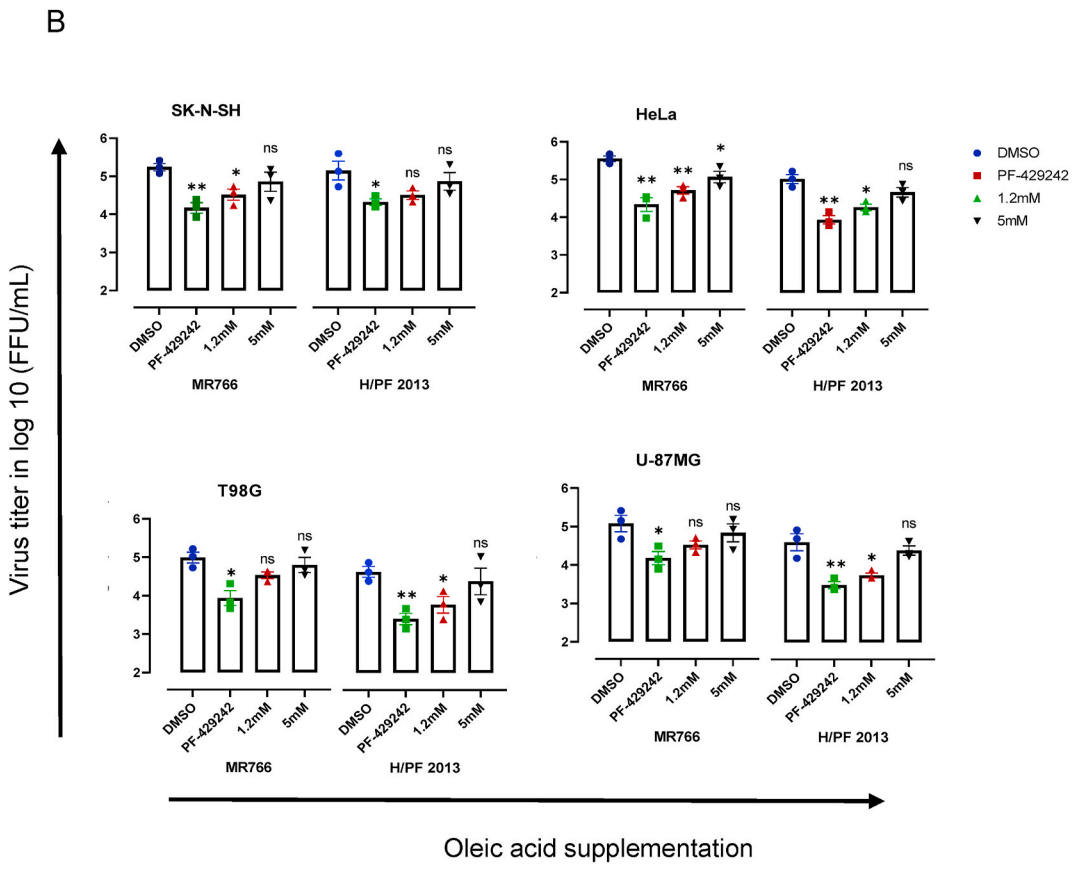

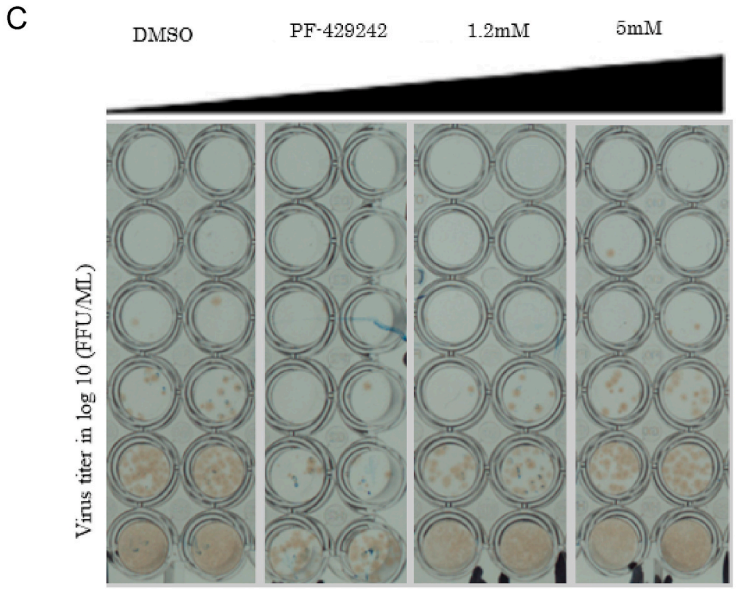

Fig. 5. (*continued*).

supplementation, as demonstrated by (Fujimoto et al., 2006); Rohweddder et al. (2014). Our data from imaging of lipid droplet showed that ZIKV protein co-localise with lipid droplet. This result not only confirm that lipid droplets are a major platform for ZIKV replication but also it effectively increases ZIKV titer in infected cells.

Treatment with both statin inhibitors resulted in a significant reduction of the ZIKV titer; however, fenofibrate reduced ZIKV replication markedly more than lovastatin (Fig. 6A). Similarly, fenofibrate reduced severe fever with thrombocytopenia syndrome virus more efficiently than lovastatin at 48 HPIs in a study conducted by (Urata et al., 2018). The ability of fenofibrate to decrease ZIKV replication in cultured cells—in contrast to lovastatin—clearly highlights the involvement of lipid droplets in ZIKV infection. The difference in anti-ZIKV activity exhibited by these statins likely stems from variation

Table 2
Cytotoxic effects of cholesterol on cell viability.

Cell line	Cholesterol
	CC_{50}% (250x dilution)
SK-N-SH	100
HeLa	98
T98G	95
U-87MG	100

in their chemical structure (Españo et al., 2019). It has been reported that therapeutic agents targeting distinct molecular pathways crucial for the pathogen replication cycle are essential for minimising drug resistance (O. Achieng et al., 2017). Thus, the novelty of PF-429242—given its ability to target SREBP, which is involved in both lipid metabolism and cellular processes such as autophagy (Cheng et al., 2018), membrane biogenesis (Castoreno et al., 2005), and excitotoxicity (Taghibiglou et al., 2009)—makes it an attractive and promising compound for use against ZIKV infection. Furthermore, the inhibition of SREBP suppresses genome replication in related viruses such as West Nile virus (Merino-Ramos et al., 2017), dengue virus (Uchida et al., 2016), Hepatitis B virus and Hepatitis C virus (Wu et al., 2018), demonstrating the potential broad spectrum of antiviral therapies based on inhibiting lipid metabolism. In conclusion, the desirable ability of PF-429242 to suppress ZIKV infection in neuronal cell lines offers potential for repurposing this inhibitor as an antiviral drug against ZIKV infection.

Funding

This research was supported by Japan Agency of Medical Research and Development (AMED) under Grant Number JP20wm0125006 and

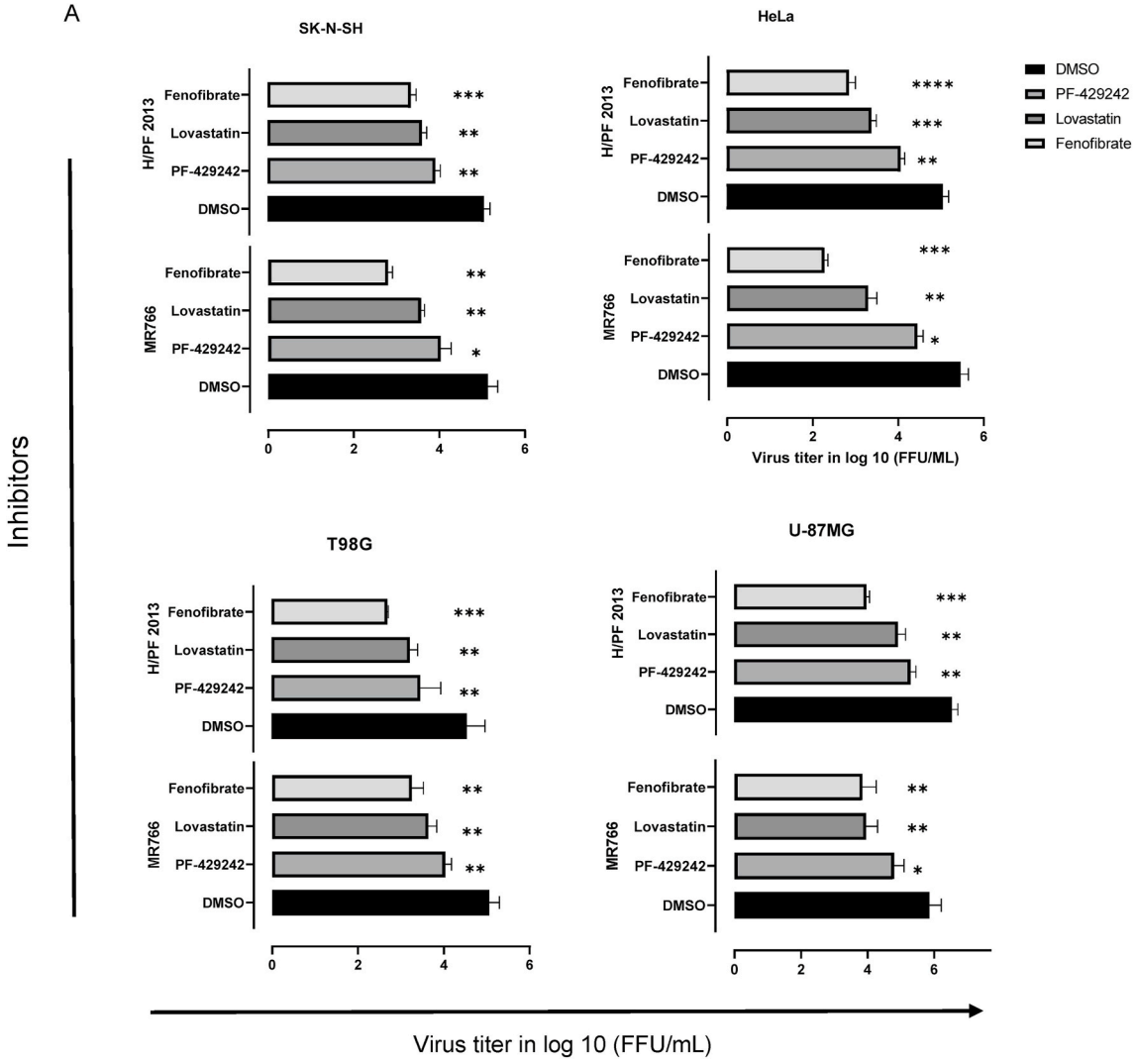

Fig. 6. Lipid droplet play a significant role in ZIKV infection. Cells at a density of 2×10^5 cells per well were seeded in a 24-well plate and infected with $ZIKV_{MR\text{-}766}$ and $ZIKV_{H/PF\ 2013}$ at MOI of 0.1 in a culture medium containing 12 μM of PF-429242 or DMSO. After 24 h incubation, the culture media were replaced with fresh media containing 40 μM of lovastatin or fenofibrate. The culture supernatants were harvested at 48 h to measure the virus titer via immunostaining. Fenofibrate inhibitor resulted in significant reduction of ZIKV titer by focus reduction assay as compared to lovastatin inhibitor (Fig. 6A). Fig. 6B shows representative photomicrographs of infected and uninfected HeLa cells. HeLa cells were exposed to ZIKV infection at 12 μM or DMSO in presence of oleic acid for 24 HPI. ZIKV E protein was detected by Alexa Fluor 594-anti-mouse IgG antibody (Invitrogen) with 2.5 μM/ml of BODIPY 493/503. Images of DAPI staining of nucleus (blue), LD (green), E-protein (red) and overlay (merged images of blue, green, and red) are shown. Co-localization of green (LD) and red (ZIKV E-protein was observed, thus confirming that lipid droplets are a major platform for ZIKV replication. Images were captured using BZ-X710 fluorescence microscope with 20x objective. Fluorescence intensity was measured at Ex 485 nm and E515 nm Fig. 6C. The asterisks indicate statistical significance in comparison to DMSO, as follows: *, $P < 0.05$; **, P 0.005. The SEM values of the results from three independent experiments are shown.

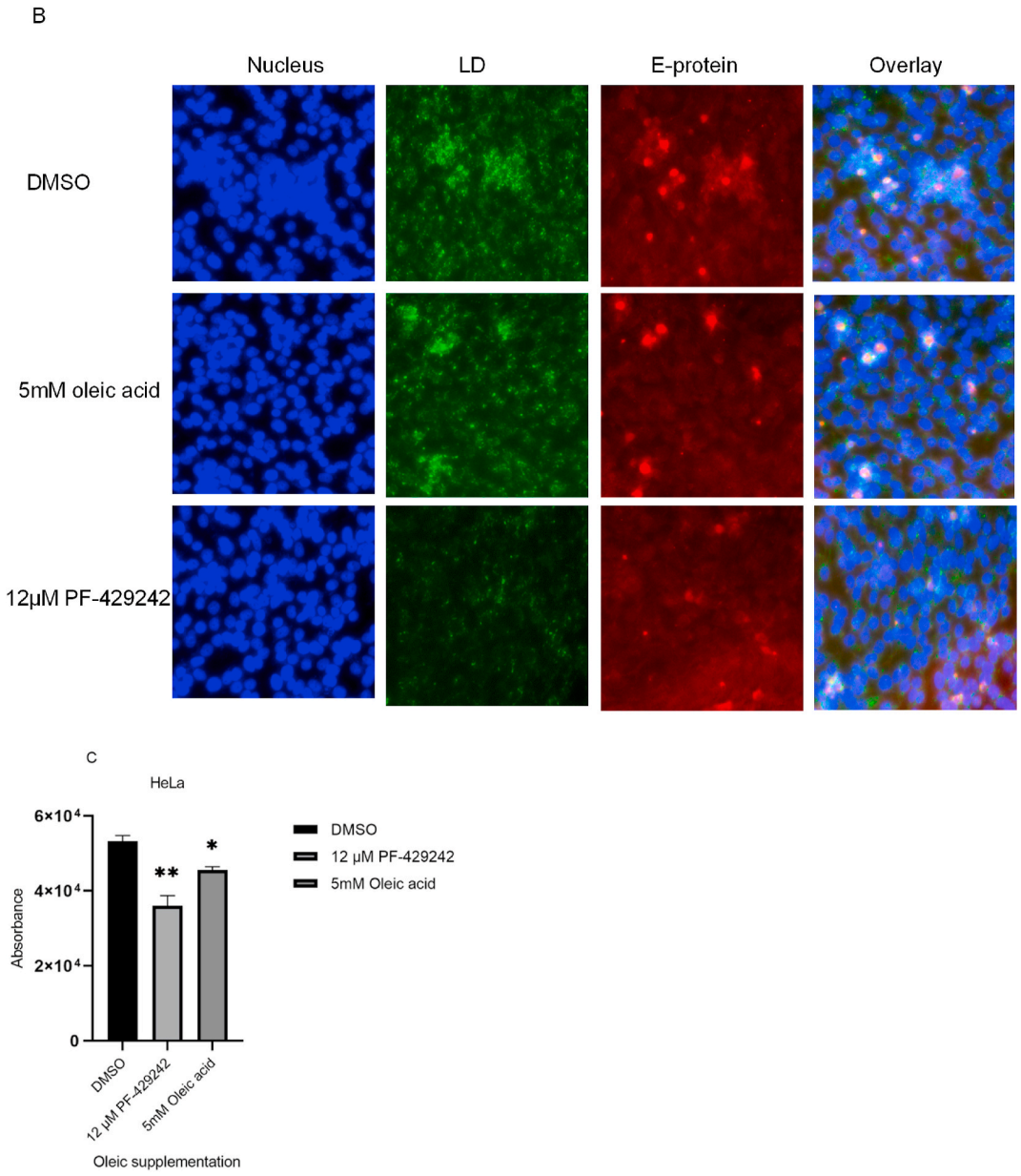

Fig. 6. (*continued*).

Table 3
Cytotoxic effects of Fenofibrate and Lovastatin on cell viability.

Cell line	Fenofibrate	Lovastatin
	$CC_{50\mu M}$	$CC_{50\mu M}$
SK-N-SH	63	81
HeLa	87	79
T98G	71	95
U-87MG	125	141

$CC_{50\mu M}$ (Concentration causing 50% reduction in cell survival).

JP21wm0225017 (Japan program for Infectious Diseases Research and Infrastructure).

Declaration of competing interest

The authors declare that they have no known competing financial interests or personal relationships that could have appeared to influence the work reported in this paper.

Acknowledgements

We would like to acknowledge the valuable scientific contributions of Tsuyoshi Ando and Jalal Alshaweesh. We are also grateful to all the members of the Department of virology, Institute of Tropical Medicine, Nagasaki University. R.S.K. is a recipient of Japan International Cooperation Agency (JICA) scholarship and is grateful for academic support from the program for Nurturing Global Leaders in Tropical and Emerging Communicable Diseases of Graduate School of Biomedical Sciences, Nagasaki University. The graphical abstract was created with BioRender.com.

Appendix A. Supplementary data

Supplementary data related to this article can be found at https://doi.org/10.1016/j.antiviral.2021.105121.

References

Achieng, O.,]wat, M., Ogutu, B., Guyah, B., Michael Ong'echa, J., Perkins, J.D., Kempaiah, P., 2017. Antimalarials: molecular drug targets and mechanism of action. Curr. Top. Med. Chem. 17 https://doi.org/10.2174/1568026617666170130115323.

Adcock, R.S., Chu, Y.K., Golden, J.E., Chung, D.H., 2017. Evaluation of anti-Zika virus activities of broad-spectrum antivirals and NIH clinical collection compounds using a cell-based, high-throughput screen assay. Antivir. Res. 138, 47–56. https://doi.org/10.1016/j.antiviral.2016.11.018.

Alipour, F., Hassanabadi, A., 2012. Effects of sterol regulatory element-binding protein (SREBP) in chickens. Lipids Health Dis. 11, 1–7. https://doi.org/10.1186/1476-511X-11-20.

Arul, M., 2017. Heterogeneity in cancer cells : variation in drug response in different primary and secondary colorectal cancer cell lines in vitro. In Vitro Cell. Develop. Biol. - Animal 435–447. https://doi.org/10.1007/s11626-016-0126-x.

Balasubramanian, A., Teramoto, T., Kulkarni, A.A., Bhattacharjee, A.K., Padmanabhan, R., 2017. Antiviral activities of selected antimalarials against dengue virus type 2 and Zika virus. Antivir. Res. 137, 141–150. https://doi.org/10.1016/j.antiviral.2016.11.015.

Blanchet, M., Seidah, N.G., Labonté, P., 2012. SKI-1/S1P inhibition: a promising surrogate to statins to block Hepatitis C virus replication. Antivir. Res. 95, 159–166. https://doi.org/10.1016/j.antiviral.2012.05.006.

Blanchet, M., Sureau, C., Guévin, C., Seidah, N.G., Labonté, P., 2015. SKI-1/S1P inhibitor PF-429242 impairs the onset of HCV infection. Antivir. Res. 115, 94–104. https://doi.org/10.1016/j.antiviral.2014.12.017.

Castoreno, A.B., Wang, Y., Stockinger, W., Jarzylo, L.A., Du, H., Pagnon, J.C., Shieh, E.C., Nohturfft, A., 2005. Transcriptional regulation of phagocytosis-induced membrane biogenesis by sterol regulatory element binding proteins. Proc. Natl. Acad. Sci. U. S. A 102, 13129–13134. https://doi.org/10.1073/pnas.0506716102.

Chan, J.F.W., Yip, C.C.Y., Tsang, J.O.L., Tee, K.M., Cai, J.P., Chik, K.K.H., Zhu, Z., Chan, C.C.S., Choi, G.K.Y., Sridhar, S., Zhang, A.J., Lu, G., Chiu, K., Lo, A.C.Y., Tsao, S.W., Kok, K.H., Jin, D.Y., Chan, K.H., Yuen, K.Y., 2016. Differential cell line susceptibility to the emerging Zika virus: implications for disease pathogenesis, non-vector-borne human transmission and animal reservoirs. Emerg. Microb. Infect. 5, e93 https://doi.org/10.1038/emi.2016.99.

Chan, J.F.W., Chik, K.K.H., Yuan, S., Yip, C.C.Y., Zhu, Z., Tee, K.M., Tsang, J.O.L., Chan, C.C.S., Poon, V.K.M., Lu, G., Zhang, A.J., Lai, K.K., Chan, K.H., Kao, R.Y.T., Yuen, K.Y., 2017. Novel antiviral activity and mechanism of bromocriptine as a Zika virus NS2B-NS3 protease inhibitor. Antivir. Res. 141, 29–37. https://doi.org/10.1016/j.antiviral.2017.02.002.

Cheng, C., Deng, X., Xu, K., 2018. Increased expression of sterol regulatory element binding protein-2 alleviates autophagic dysfunction in NAFLD. Int. J. Mol. Med. 41, 1877–1886. https://doi.org/10.3892/ijmm.2018.3389.

Chiu, H.P., Chiu, H., Yang, C.F., Lee, Y.L., Chiu, F.L., Kuo, H.C., Lin, R.J., Lin, Y.L., 2018. Inhibition of Japanese encephalitis virus infection by the host zinc-finger antiviral protein. PLoS Pathog. 14, 1–23. https://doi.org/10.1371/journal.ppat.1007166.

Delvecchio, R., Higa, L.M., Pezzuto, P., Valadão, A.L., Garcez, P.P., Monteiro, F.L., Loiola, E.C., Dias, A.A., Silva, F.J.M., Aliota, M.T., Caine, E.A., Osorio, J.E., Bellio, M., O'Connor, D.H., Rehen, S., De Aguiar, R.S., Savarino, A., Campanati, L., Tanuri, A., 2016. Chloroquine, an endocytosis blocking agent, inhibits zika virus infection in different cell models. Viruses 8, 1–15. https://doi.org/10.3390/v8120322.

Españo, E., Nam, J.H., Song, E.J., Song, D., Lee, C.K., Kim, J.K., 2019. Lipophilic statins inhibit Zika virus production in Vero cells. Sci. Rep. 9, 1–11. https://doi.org/10.1038/s41598-019-47956-1.

Fujimoto, Y., Onoduka, J., Homma, K.J., Yamaguchi, S., Mori, M., Higashi, Y., Makita, M., Kinoshita, T., Noda, J.I., Itabe, H., Takano, T., 2006. Long-chain fatty acids induce lipid droplet formation in a cultured human hepatocyte in a manner dependent of acyl-CoA synthetase. Biol. Pharm. Bull. 29, 2174–2180. https://doi.org/10.1248/bpb.29.2174.

González, M.C.B., Menichetti, E., Geretschläger, R., Gabriel, C., Simon, V., Lim, J.K., 2018. Tick-borne encephalitis virus vaccine-induced human antibodies mediate negligible enhancement of zika virus infection in vitro and in a mouse model James. mSphere 3, 1–10. https://doi.org/10.1128/mSphereDirect.00011-18.

Heaton, N.S., Randall, G., 2011. Multifaceted roles for lipids in viral infection. Trends Microbiol. 19, 368–375. https://doi.org/10.1016/j.tim.2011.03.007.

Hyrina, A., Meng, F., McArthur, S.J., Eivemark, S., Nabi, I.R., Jean, F., 2017. Human Subtilisin Kexin Isozyme-1 (SKI-1)/Site-1 Protease (S1P) regulates cytoplasmic lipid droplet abundance: a potential target for indirect-acting anti-dengue virus agents. PloS One 12, 1–22. https://doi.org/10.1371/journal.pone.0174483.

Komoto, S., Fukuda, S., Murata, T., Taniguchi, K., 2020. Reverse genetics system for human rotaviruses. Microbiol. Immunol. 64, 401–406. https://doi.org/10.1111/1348-0421.12795.

Kuivanen, S., Bespalov, M.M., Nandania, J., Ianevski, A., Velagapudi, V., De Brabander, J.K., Kainov, D.E., Vapalahti, O., 2017. Obatoclax, saliphenylhalamide and gemcitabine inhibit Zika virus infection in vitro and differentially affect cellular signaling, transcription and metabolism. Antivir. Res. 139, 117–128. https://doi.org/10.1016/j.antiviral.2016.12.022.

Lee, C.-J., Lin, H.-R., Liao, C.-L., Lin, Y.-L., 2008. Cholesterol effectively blocks entry of flavivirus. J. Virol. 82, 6470–6480. https://doi.org/10.1128/jvi.00117-08.

Lessler, J., Chaisson, L.H., Kucirka, L.M., Bi, Q., Grantz, K., Salje, H., Carcelen, A.C., Ott, C.T., Sheffield, J.S., Neil, M., Cummings, D.A.T., Metcalf, C.J.E., Rodriguez, I., 2017. HHS Publ. Access 353, 1–25. https://doi.org/10.1126/science.aaf8160. Assessing.

Majeed, Y., Upadhyay, R., Alhousseiny, S., Taha, T., Musthak, A., Shaheen, Y., Jameel, M., Triggle, C.R., Ding, H., 2019. Potent and PPARα-independent anti-proliferative action of the hypolipidemic drug fenofibrate in VEGF-dependent angiosarcomas in vitro. Sci. Rep. 9, 1–14. https://doi.org/10.1038/s41598-019-42838-y.

Martín-Acebes, M.A., Vázquez-Calvo, Á., Saiz, J.C., 2016. Lipids and flaviviruses, present and future perspectives for the control of dengue, Zika, and West Nile viruses. Prog. Lipid Res. 64, 123–137. https://doi.org/10.1016/j.plipres.2016.09.005.

McNab, F., Mayer-Barber, K., Sher, A., Wack, A., O'Garra, A., 2015. Type I interferons in infectious disease. Nat. Rev. Immunol. 15, 87–103. https://doi.org/10.1038/nri3787.

Merino-Ramos, T., Jiménez De Oya, N., Saiz, J.C., Martín-Acebes, M.A., 2017. Antiviral activity of nordihydroguaiaretic acid and its derivative tetra-O-methyl nordihydroguaiaretic acid against West Nile virus and Zika virus. Antimicrob. Agents Chemother. 61, 1–10. https://doi.org/10.1128/AAC.00376-17.

Miner, J.J., Diamond, M.S., 2017. Zika virus pathogenesis and tissue tropism. Cell Host Microbe 21, 134–142. https://doi.org/10.1016/j.chom.2017.01.004.

Osuna-Ramos, J.F., Reyes-Ruiz, J.M., Del Ángel, R.M., 2018. The role of host cholesterol during flavivirus infection. Front. Cell. Infect. Microbiol. 8, 388. https://doi.org/10.3389/fcimb.2018.00388.

Ramphan, S., Suksathan, S., Wikan, N., Ounjai, P., Boonthaworn, K., Rimthong, P., Kanjanapruthipong, T., Worawichawong, S., Jongkaewwattana, A., Wongsiriroj, N., Smith, D.R., 2017. Oleic acid enhances dengue virus but not dengue virus-like particle production from mammalian cells. Mol. Biotechnol. 59, 385–393. https://doi.org/10.1007/s12033-017-0029-4.

Ringseis, R., Rauer, C., Rothe, S., Gessner, D.K., Schütz, L.M., Luci, S., Wen, G., Eder, K., 2013. Sterol regulatory element-binding proteins are regulators of the NIS gene in thyroid cells. Mol. Endocrinol. 27, 781–800. https://doi.org/10.1210/me.2012-1269.

Rohwedder, A., Zhang, Q., Rudge, S.A., Wakelam, M.J.O., 2014. Lipid droplet formation in response to oleic acid in Huh-7 cells is mediated by the fatty acid receptor FFAR4. J. Cell Sci. 127, 3104–3115. https://doi.org/10.1242/jcs.145854.

Rumlová, M., Ruml, T., 2020. Since January 2020 Elsevier Has Created a COVID-19 Resource Centre with Free Information in English and Mandarin on the Novel Coronavirus COVID- 19 . The COVID-19 Resource Centre Is Hosted on Elsevier Connect. the company ' s public news and information.

Schwarz, M.C., Sourisseau, M., Espino, M.M., Gray, E.S., Chambers, M.T., Tortorella, D., Evans, M.J., 2016. Rescue of the 1947 zika virus prototype strain with a cytomegalovirus promoter-driven cDNA clone. mSphere 1, 1–12. https://doi.org/10.1128/msphere.00246-16.

Simonin, Y., Loustalot, F., Desmetz, C., Foulongne, V., Constant, O., Fournier-Wirth, C., Leon, F., Molès, J.P., Goubaud, A., Lemaitre, J.M., Maquart, M., Leparc-Goffart, I., Briant, L., Nagot, N., Van de Perre, P., Salinas, S., 2016. Zika virus strains potentially display different infectious profiles in human neural cells. EBioMedicine 12, 161–169. https://doi.org/10.1016/j.ebiom.2016.09.020.

Song, B.H., Yun, S.I., Woolley, M., Lee, Y.M., 2017. Zika virus: history, epidemiology, transmission, and clinical presentation. J. Neuroimmunol. 308, 50–64. https://doi.org/10.1016/j.jneuroim.2017.03.001.

Song, W., Zhang, H., Zhang, Y., Li, R., Han, Y., Lin, Y., Jiang, J., 2020. Repurposing clinical drugs is a promising strategy to discover drugs against Zika virus infection. Front. Med. https://doi.org/10.1007/s11684-021-0834-9.

Taghibiglou, C., Martin, H.G.S., Lai, T.W., Cho, T., Prasad, S., Kojic, L., Lu, J., Liu, Y., Lo, E., Zhang, S., Wu, J.Z.Z., Li, Y.P., Wen, Y.H., Imm, J.H., Cynader, M.S., Wang, Y. T., 2009. Role of NMDA receptor-dependent activation of SREBP1 in excitotoxic and ischemic neuronal injuries. Nat. Med. 15, 1399–1406. https://doi.org/10.1038/nm.2064.

Talarico, L.B., Pujol, C.A., Zibetti, R.G.M., Faría, P.C.S., Noseda, M.D., Duarte, M.E.R., Damonte, E.B., 2005. The antiviral activity of sulfated polysaccharides against dengue virus is dependent on virus serotype and host cell. Antivir. Res. 66, 103–110. https://doi.org/10.1016/j.antiviral.2005.02.001.

Teissier, E., Penin, F., Pécheur, E.I., 2011. Targeting cell entry of enveloped viruses as an antiviral strategy. Molecules 16, 221–250. https://doi.org/10.3390/molecules16010221.

Tun, M.M.N., Zin, K., Inoue, S., Kurosawa, Y., Lwin, Y.Y., Lin, S., Aye, K.T., Khin, P.T., Myint, T., Htwe, K., Mapua, C.A., Natividad, F.F., Hirayama, K., Kouichi, M., 2013. Serological characterization of dengue virus infections observed among dengue hemoharrgic fever/dengue shock syndrome cases in Upper Myanmar. J. Med. Virol. 851258–1266 Serol. 55, 52–55. https://doi.org/10.1002/jmv.

Tun, M.M.N., Aoki, K., Senba, M., Buerano, C.C., Shirai, K., Suzuki, R., Morita, K., Hayasaka, D., 2014. Protective role of TNF-α, IL-10 and IL-2 in mice infected with the Oshima strain of Tick-borne encephalitis virus. Sci. Rep. 4, 1–9. https://doi.org/10.1038/srep05344.

Uchida, L., Urata, S., Ulanday, G.E.L., Takamatsu, Y., Yasuda, J., Morita, K., Hayasaka, D., 2016. Suppressive effects of the site 1 protease (S1p) inhibitor, PF-429242, on dengue virus propagation. Viruses 8, 1–12. https://doi.org/10.3390/v8020046.

Urata, S., Yun, N., Pasquato, A., Paessler, S., Kunz, S., de la Torre, J.C., 2011. Antiviral activity of a small-molecule inhibitor of arenavirus glycoprotein processing by the cellular site 1 protease. J. Virol. 85, 795–803. https://doi.org/10.1128/jvi.02019-10.

Urata, S., Uno, Y., Kurosaki, Y., Yasuda, J., 2018. The cholesterol, fatty acid and triglyceride synthesis pathways regulated by site 1 protease (S1P) are required for efficient replication of severe fever with thrombocytopenia syndrome virus. Biochem. Biophys. Res. Commun. 503, 631–636. https://doi.org/10.1016/j.bbrc.2018.06.053.

Wang, L., Liang, R., Gao, Y., Li, Y., Deng, X., Xiang, R., Zhang, Y., Ying, T., Jiang, S., Yu, F., 2019. Development of small-molecule inhibitors against zika virus infection. Front. Microbiol. 10, 1–21. https://doi.org/10.3389/fmicb.2019.02725.

Wu, Q., Li, Z., Liu, Q., 2018. An important role of SREBP-1 in HBV and HCV co-replication inhibition by PTEN. Virology 520, 94–102. https://doi.org/10.1016/j.virol.2018.05.011.

Xu, M.Y., Liu, S.Q., Deng, C.L., Zhang, Q.Y., Zhang, B., 2016. Detection of Zika virus by SYBR green one-step real-time RT-PCR. J. Virol. Methods 236, 93–97. https://doi.org/10.1016/j.jviromet.2016.07.014.